



HAL
open science

Tailoring 3-component photoinitiating systems for use as efficient photopolymerizable holographic material

Ahmad Ibrahim, Christian Ley, Xavier Allonas, Christiane Carré, Isabelle Pillin

► To cite this version:

Ahmad Ibrahim, Christian Ley, Xavier Allonas, Christiane Carré, Isabelle Pillin. Tailoring 3-component photoinitiating systems for use as efficient photopolymerizable holographic material. Journal of Display Technology, 2014, 10 (6), pp.456. 10.1109/JDT.2014.2314863 . hal-01020980

HAL Id: hal-01020980

<https://hal.science/hal-01020980>

Submitted on 17 Jul 2014

HAL is a multi-disciplinary open access archive for the deposit and dissemination of scientific research documents, whether they are published or not. The documents may come from teaching and research institutions in France or abroad, or from public or private research centers.

L'archive ouverte pluridisciplinaire **HAL**, est destinée au dépôt et à la diffusion de documents scientifiques de niveau recherche, publiés ou non, émanant des établissements d'enseignement et de recherche français ou étrangers, des laboratoires publics ou privés.

Tailoring 3-component photoinitiating systems for use as efficient photopolymerizable holographic material

Ahmad Ibrahim¹, Christian Ley¹, Xavier Allonas¹, Christiane Carré² and I. Pillin³

- (1) Laboratory of Photochemistry and Macromolecular Engineering, Université de Haute Alsace, ENSCMu, 3 rue Alfred Werner, 68093 MULHOUSE, France
(2) CNRS, UMR 6082 FOTON, Enssat, 6 rue de Kerampont, CS 80518, 22305 LANNION Cedex, France
(3) Laboratoire d'Ingénierie des Matériaux de Bretagne (LIMATB), Université de Bretagne Sud (UBS), Centre de Recherche, BP 92116, Rue Saint Maudé, 56321 LORIENT, France

Abstract: *To enhance the efficiency of photopolymerizable systems as holographic recording materials, the use of 3-component photoinitiating systems was explored. In order to get more insight into the hologram formation, gratings' recording curves were compared to those of monomer conversion obtained by RTFTIR spectroscopy. This work outlines the differences between the photoinitiating systems. A holographic 3-component recording material giving rise to thick phase holograms with both high diffraction yield and high rate of formation is highlighted.*

Index Terms: Photopolymerization, holographic recording material, diffraction grating, optical storage.

I- INTRODUCTION

An ever-increasing number of photosensitive organic materials were and are always being examined for the fields of photonics and information displays (diffractive optical elements, narrowband optical filters, optical interconnects, waveguide couplers, three-dimensional displays or holographic memories) [1]-[4], due to the possibility of structuration of the matter by the light in the micro and nanometer range. Particularly, there is a growing need to increase the capabilities of photosensitive polymer used as holographic data storage systems (large refractive index changes, high spatial resolution, dry processing capability, form flexibility, reduced costs).

In holography, a photopolymerizable recording medium consists of a homogeneous mixture of different monomers generally associated to a bimolecular PIS (photoinitiating system): a photoinitiator and a coinitiator (2-component systems). The writing process is based on two interfering laser beams creating an interference pattern. In these conditions, free radicals are inhomogeneously generated by photoreaction between the excited dye and the coinitiator. The result is a photoinitiated polymerization occurring at different rates in the bright and dark areas [4], [5]. Then, formation of spatial concentration gradients of monomer leads in turn to mass diffusion process, giving rise to a modulation of refractive index or thickness in the final material.

Formulating of such material requires a fair knowledge of the different processes taking place during irradiation, particularly of the coupling between photochemical conversion, mass transport and stiffening of the polymer matrix, which is not a straightforward matter. This insight is needed to optimize the customization of the material, to define its best conditions of use and to meet the required specifications.

On the other hand, photopolymerization technology has gained prominence as an attractive alternative to traditional polymerization processes due to variety of advantages and benefits. These profits can be attributed to the use of energy of light, rather than thermal energy to induce polymerization reactions. As an efficient, low cost, and environmentally favorable method, photopolymerization has led to remarkable expansion in a variety of applications: coatings, adhesives, composites, image science, microelectronic, optics industries, biomedical arena and the fabrication of three-dimensional prototype [6]-[10].

Many different PIS are available covering a wide range of applications. To give sensitivity into

visible range of the electromagnetic spectrum, bimolecular systems are proposed. In that case, the chromophore's excited state reached after light absorption reacts with a co-initiator, to give rise to radicals and to initiate polymerization of the medium [6], [11], [12]. These systems can be used as holographic polymer recording materials [13]-[15]. Being less efficient than the PIS molecule able to dissociate into radicals after UV light absorption, different methods have been proposed to enhance their efficiency. Among them, the use of additional redox additives leads to the so-called three-component photoinitiating systems [16]. These systems consist in a light absorbing chromophore (the dye), an electron donor/acceptor as co-initiator and a third component. Many works and results have proved that these 3-component PIS are faster and more efficient than the corresponding two component systems [17]-[21]. In addition, the dyes in these photoinitiating systems can undergo easily complete photobleaching reaction during the photopolymerization [22] which is of importance for holographic recording materials in order to obtain clear optical devices. The use of 3-component PIS based on boron-dipyrromethene dye [23], [24] for holographic recording was recently outlined [25].

Therefore, 3-component PIS could be of great importance in the purpose of highly efficient and specific holographic materials: i- the higher sensitivity of these system could results in less dye into formulation leading to better optical clearness of final devices, ii- the way to tune the photoresponse properties of the hologram material makes possible the choice between high final diffraction efficiency or fast hologram formation.

In this paper, the efficiency of two 3-component PIS as holographic recording material is analyzed in term of photopolymerization kinetics and diffraction yield. The selected systems are based on a dye, an amine as electron donor and a bisimidazole derivative (HABI) as the third component. In order to investigate the influence of the photophysical properties of dye on the holographic recording material performance, two different dyes (Rose Bengal (RB) and Safranin O (SFH⁺)) are experimentally examined. Simultaneously, these visible curable systems are associated to fluorinated acrylate monomers for the recording of transmission gratings. The partial fluorination of host polymer matrices results in improved optical properties with an enhancement in contrast ratio and better defined morphologies [26], [27].

II- EXPERIMENTAL

All experiments were performed at 20°C (preparation of the samples, RT-FTIR and holographic recordings).

A- Chemicals

In the interest of speed and economy, Rose Bengal (RB), Safranin O (SFH⁺), 2,2'-Bis(2-Chlorophenyl)-4,4',5,5'-tetraphenyl-1,2'-biimidazole (CIHABI) and *N*-Phenylglycine (NPG) were purchased from Aldrich. Their chemical structures are shown in Table I.

The holographic resin was a liquid mixture of different monomers and additives. The choice of the formulation was governed by earlier experiments performed in the field of visible curable systems and use of fluorinated acrylate monomers for the recording of holographic polymer-dispersed liquid crystals (LC) transmission gratings [28], [29]:

- 45 wt % of a hexafunctional aliphatic urethane acrylate oligomer (Ebecryl 1290, Cytec) acting as primary oligomer;
- 22.5 wt % of 1,1,1,3,3,3-hexafluoroisopropyl acrylate and 22.5 wt% of vinyl neonanoate, both from Aldrich. The vinyl ester monomer is known to copolymerize very easily with acrylic monomers[27];
- 5 wt % of *N*-vinyl pyrrolidinone (Aldrich) which is a standard additive introduced in phopolymerizable systems here to favor compounds solubility [30];
- 5 wt % of trimethylolpropane tris(3-mercaptopropionate) (Aldrich) which is a trifunctional thiol able to increase the photopolymerization rate in air and leading to higher monomer conversions [30].

For all experiments, the photoinitiating system compounds were introduced in the holographic resin

in the following weight ratio: 0.2 wt% of dye (RB or SFH⁺), 0.6 wt% of electron donor (NPG) and 1 wt% of electron acceptor (CIHABI). The maximum absorption for RB and SFH⁺ are respectively at 560 and 516 nm. At 514 nm, the RB absorption is three times lower than those of SFH⁺. In addition, the two dyes are different: RB is an electron rich, negatively charged compound whereas SFH⁺ is an electron deficient positive charged compound.

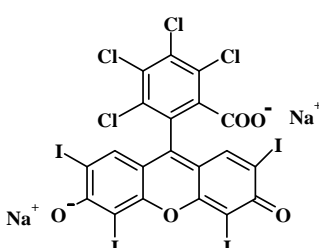
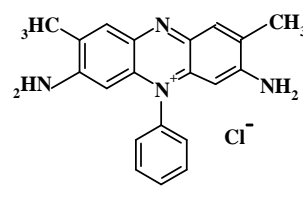
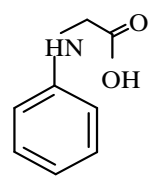
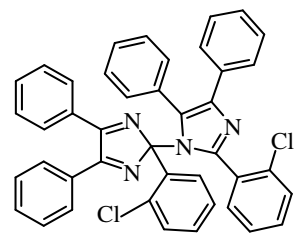
Dyes	
	
Rose Bengal (RB)	Safranin O (SF+)
Co initiators	
	
N-phenylglycine (NPG)	CIHABI

Table 1: Molecular structures of the dyes used in this study.

B- RT-FTIR measurements

The study of photopolymerization kinetics was carried out by RT-FTIR (real time fourier transform infrared) spectroscopy using a Vertex 70 FTIR spectrophotometer (Bruker Optik), equipped with a MCT detector working in the rapid scan mode. This allows an average of 4 scans/s collection rate using a resolution of 4 cm⁻¹. The IR spectra were then recorded during sample irradiation using a green laser diode emitting at 532 nm (Roithner Lasertechnik, 50 mW) which was adapted to the FTIR spectrometer by means of a light guide. The irradiance was adjusted at 22.5 mW/cm² on the sample. To prevent the diffusion of oxygen into the sample during the irradiation, experiments were carried out by laminating the resin between two polypropylene films and two CaF₂ windows. The thickness of the sample was adjusted using a 25 μm Teflon spacer. The spectra were recorded between 600 and 3900 cm⁻¹.

The kinetics of the polymerization were measured by following the disappearance of the C=C bond stretching signal at 1637 cm⁻¹. The degree of monomer conversion C, directly related to the decrease of peak area at 1637 cm⁻¹, was calculated according to [31], [32]:

$$C(\%) = \frac{(A_{1637})_0 - (A_{1637})_t}{(A_{1637})_0} \times 100$$

where (A₁₆₃₇)₀ and (A₁₆₃₇)_t were the area of the IR absorption band at 1637 cm⁻¹ of the sample before exposure and at time t respectively. A good estimate of the maximum rate of conversion R'_p was determined by the slope of the conversion kinetics at the inflection point. The conversion rate R'_p is linearly related to the rate of polymerization R_p by R'_p = R_p × 100/[M₀] where [M₀] is the initial monomer concentration (i.e. before exposure). According to this linear relationship, the values of conversion rate R'_p are reported in this work [32].

C- Holographic recording

The samples were prepared by embedding the photopolymerizable formulation between two glass-substrates. Calibrated glass beads were used as spacers to guarantee the thickness of the system around 20 μm . During holographic recording with a 514 nm actinic laser light (Coherent Innova 308C Argon Ion laser), a sinusoidal light pattern was generated by interference of two incident plane waves, the angle between the two interfering beams being of ca 33° (Fig. 1) [4], [33]. The choice of this writing wavelength was in good agreement with the maximum absorption of SFH⁺. As high diffraction efficiencies were recorded at 514 nm with RB-NPG [28], working simultaneously at the maximum absorption of RB was not necessary in this study. The two s-polarized beams were of equal intensity, corresponding to a total power density of 25 mW/cm² incident on the photosensitive samples for a beam diameter of 2.5 cm. The fringe spacing was adjusted to ca. 0.9 μm and total exposure duration of ca. 90 s.

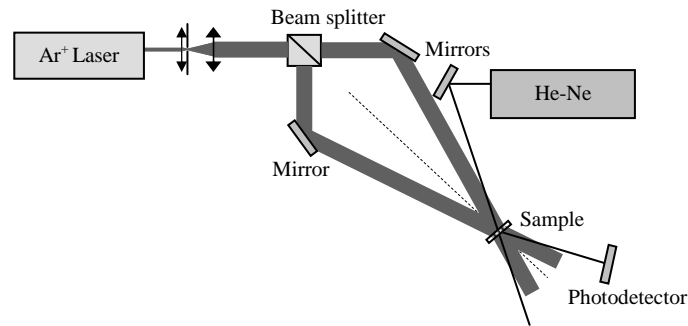


Fig. 1: Experimental set-up used for recording sinusoidal gratings in the photopolymerizable samples.

When the holographic formulations are illuminated by the sinusoidal interference pattern, inhomogeneous polymerization reaction and dye bleaching take place. Monomer and sensitizer consumption in the bright regions led to spatial concentration gradients of these molecules which, in turn, led to diffusion processes. This coupling of photochemical conversion and mass transport results in regions of different matter density. The holographic material being laminated between two windows suppressing any generation of surface relief, a modulation of the refractive index in the material is then created, giving rise to thick volume phase gratings with high diffraction efficiencies and low scattering noise [4], [28].

The fact that no chemical post-treatment was needed for this recording material, allowed the continuous follow up of the hologram formation process during exposure by use of an inactinic reading light beam (633 nm HeNe laser) which is more or less diffracted (Fig. 1). The diffraction efficiency at 633 nm (η) was defined by the ratio of the intensity of the first diffraction order to the diffracted plus transmitted light intensities. This measurement instead of the ratio of the diffracted intensity by the incident intensity at 633 nm was performed in order to rule out Fresnel losses in the determination of the grating diffraction efficiency. The rate of grating formation R_η was calculated as:

$$R_\eta = \frac{d\eta}{dt}$$

D- AFM characterization

The nano-scale characterizations of polymer gratings were done using atomic force microscopy (AFM) in ambient conditions using light tapping mode (TM-AFM) on a Caliber multimode scanning probe microscope from Bruker-Veeco, France. The set point amplitude of antimony doped silicon tapping mode cantilever (LTESP model, Veeco, USA) was about 4.5 V. The cantilever with tip radius between 5 and 20 nm had typical resonance frequency about 270 kHz, and a cantilever spring constant (k) was 20-80 N/m. The morphology of polymer gratings was analysed using the SPM lab software.

III- MECHANISTIC STUDY OF THE PHOTOINITIATING SYSTEM

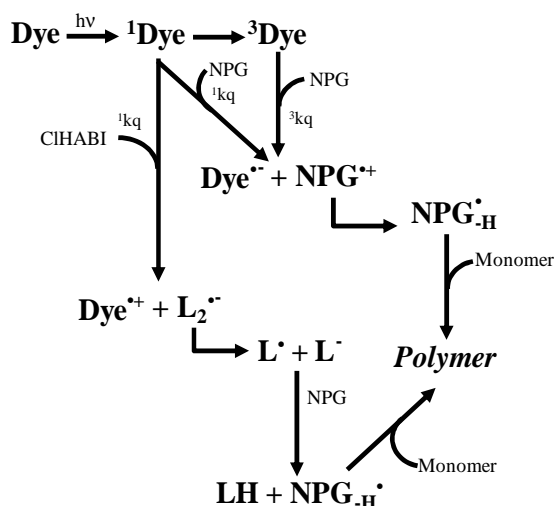
The full photochemical study of the two 3-component PIS based on RB or SFH⁺ was performed by time resolved and steady state spectroscopies (i.e. laser flash photolysis and fluorescence). The bimolecular reaction rate constants k_q of singlet and triplet states of the dyes ($^1\text{RB}/^3\text{RB}$ and $^1\text{SFH}^+/^3\text{SFH}^+$) were determined in acetonitrile. They are in good agreement with calculated Gibbs free energy variation (ΔG_{et}) of the reactions according to our redox measurements (Table II). The ΔG_{et} for photoinduced electron transfer are given by the Rehm Weller equation [34]: $\Delta G_{\text{et}} = E_{\text{ox}} - E_{\text{red}} - E^* + C$. E_{ox} and E_{red} are the half-wave oxidation and reduction potentials for the donor and the acceptor, respectively. E^* stands for the energy of the excited state. The Coulombic term C is usually neglected in polar solvent. The full study of the dyes singlet and triplet excited state reactivity being out of the scope of the present paper is not presented in details, but general procedure can be found in some of our previous studies [23]-[25].

	ΔG_{et} (eV)/ k_q ($\text{M}^{-1} \cdot \text{s}^{-1}$)	
	Singlet state	Triplet state
	^1RB	^3RB
NPG	-0.284/5.8 10^{10}	0.086/5.0 10^7
CIHABI	-0.15/2.6 10^9	0.22/< 10^4
	$^1\text{SFH}^+$	$^3\text{SFH}^+$
NPG	-0.904/1.6 10^{10}	-0.324/1.2 10^9
CIHABI	-0.18/2.5 10^{10}	0.4/< 10^6

Table 2: Gibbs free energy variation (ΔG_{et}) and rate constants of RB and SFH⁺ excited states electron transfer reactions with the coinitiator NPG and the additive CIHABI.

Following these studies, a reaction mechanism for both dyes in acetonitrile is proposed in Scheme 1. Even both of the dyes are ionic in this study, PIS reaction mechanism is similar to those proposed for neutral compound. This result was supported by laser flash photolysis experiments. In addition, the reactivity of photocyclic initiating systems based on a pyrromethene dye, an amine as electron donor and an electron acceptor for free radical photopolymerization was similarly studied using time-resolved spectroscopic experiments, real-time FTIR and holographic recording [25].

Some remarks can be underlined according to this mechanism and to the measured rate constants. It appears that CIHABI reacts mainly with dyes singlet excited states while NPG reactivity comes from triplet states. However, all these chemical reactions are bimolecular and are strongly limited by the diffusion of molecules. As a consequence due to longer lifetime of triplet state, free radical production in the holographic material occurs mainly from the excited triplet state of the dyes by reaction with the donor NPG. Moreover, taking into account the triplet states rate constants, ^3RB show a reactivity which is two orders of magnitude lower than for $^3\text{SFH}^+$, leading to lower rates of reaction and radical generation. Different singlet and triplet states of the dye could be generated, but, as they are degenerate, the global representation $S_0/S_1/T_1$ is used.



Scheme 1: General mechanism proposed for the 3-component PIS in acetonitrile solution.

IV- PHOTOPOLYMERIZATION EXPERIMENTS

The photopolymerization efficiency of the two PIS based on Dye-NPG-CIHABI was studied using the RT-FTIR technique and outlined by the change of monomer conversion degree in the matrix as a function of irradiation time (Fig. 2). The exposure was performed by mean of a 532 nm laser diode with irradiance on the sample fixed to 22.5 mW/cm².

As can be seen, the 2-component photoinitiating system RB-CIHABI shows the lowest photopolymerization efficiency with final conversion degree and maximum conversion rate respectively around 22% and 0.3 s⁻¹. This low efficiency was ascribed to the poor initiating properties noted for lophyl radical (L[•]) [35] and the poor reactivity of the ³RB (see k_q Table II) toward CIHABI. The reactivity of RB-NPG is greater with both higher maximum conversion rate (6 s⁻¹) and final conversion degree (52%), in line with a higher rate constant of reaction of ³RB toward NPG (see k_q Table II). The addition of CIHABI is beneficial to the RB-NPG PIS as both the maximum rate of conversion and final conversion degree of the monomer are increased toward 8 s⁻¹ and 63% respectively, corresponding to the best system in terms of polymerization of the monomer mixture under homogeneous irradiation.

The behavior of SFH⁺ based PIS is different. The triplet state of safranin ³SFH⁺ exhibits the higher reactivity toward NPG (and CIHABI) with the highest rate constant of reaction. Inversely, the photopolymerization results are worst than those of RB: the final monomer conversion degree is around 35%, only half of the best RB PIS performance. However, by taking a closer look to the polymerization curves, it appears that the inhibition times of SFH⁺ systems are lower by a factor of around 5 compared to RB PIS (cf. Table III). Moreover, the maximum conversion rates R'_p (except in presence of CIHABI) are very high, i.e. 16 s⁻¹ for SFH⁺-NPG. The addition of CIHABI to this last increases the speed up to 20 s⁻¹. Thus, even if the final conversion percentages of SFH⁺ PIS are somehow disappointing, these photoinitiating systems are more than two times faster than RB PIS. Lastly as for RB, the SFH⁺-CIHABI is the slowest system with R'_p equal to 1.6 s⁻¹.

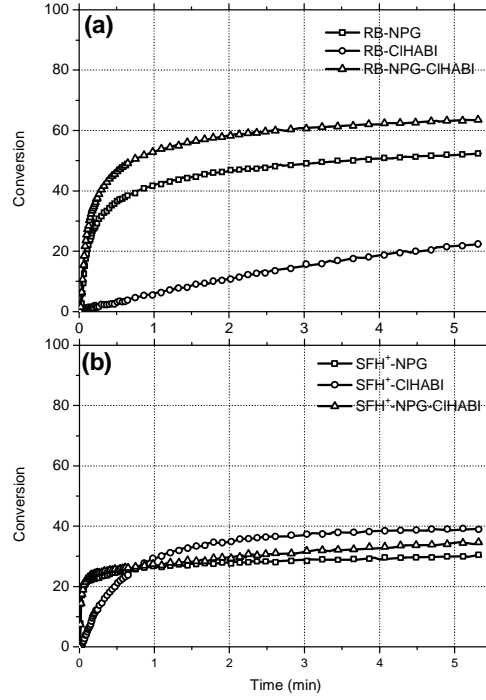


Fig. 2: Acrylate conversion (%) curves of PIS based on RB (a) and on SFH⁺ (b) upon laser exposure at 532 nm (irradiance = 22.5 mW/cm²). The values of inhibition time (t_{inh}), maximum conversion rate (R'_p) and final conversion degree (C_{max}) of monomer are collected in Table III.

Run	t_{inh} (s)	R'_p (s ⁻¹)	C_{max} (%)	t_{inh}^h (s)	η_f	R_η (s ⁻¹)
RB-NPG	1.4	6.0	52	∞	0.78	0.25
RB-CIHABI	7.8	0.3	22	1.5	0	0
RB-NPG-CIHABI	1.0	8	63	0.5	0.4	0.27
SFH ⁺ -NPG	0.2	16.0	30	0.5	0.95	0.41
SFH ⁺ -CIHABI	2.0	1.6	39	5.5	0.88	0.12
SFH ⁺ -NPG-CIHABI	0.2	20.0	34	n.m.	0.95	0.55

Table 3: Characteristic parameters for RB and SFH⁺ (parameters determined: - by RT-FTIR during photopolymerization at 532 nm for an irradiance of 22.5 mW/cm² (t_{inh} : inhibition time, R'_p : maximum conversion rate, C_{max} : final conversion degree); - by grating recording at 514 nm for an irradiance of 25 mW/cm² (t_{inh}^h : inhibition time, η_f : final diffraction efficiency, R_η : maximum rate of grating formation)).

It is interesting to note that the maximum conversion rates of the four presented 2-component systems are in line with the excited states reactivity given by the reaction rate constant k_q (Table II) determined by time resolved spectroscopy techniques: the higher the k_q , the higher the R'_p . Moreover, the maximum conversion rates obtained for the 3-component PIS are higher than the direct sum of 2-component PIS R'_p . This result outlines that the pairing of a donor co-initiator with a third acceptor component is more efficient than awaited by the addition of individual reactivities. Furthermore, inhibition times (t_{inh} = the polymerization started up after a certain time, related to the amount of oxygen dissolved in the medium) of RB and SFH⁺ systems decrease with the rates of monomer

conversion, indicating that it could be related to the speed of radicals formation from excited states of the dyes. For 3-component PIS, quenching of the excited dye is more efficient and more radicals able to initiate the polymerization of the different monomers are created in the medium. The result is a more efficient reaction than for 2-component systems.

It is tempting to ascribe the low final conversion of the fast SFH⁺ systems to a very soon and rapid gelation of the monomer mixture leading to a decrease of overall reactivity. This can be due to the use of a hexafunctional acrylate monomer which normally leads to fast reticulation and very fast increase of the viscosity in the matrix. If the slowest system for SFH⁺ (i.e. SFH⁺-CIHABI) leads to slightly higher final conversion than the two other, the comparison with RB system does not support this statement: the fastest RB-NPG-CIHABI system leads to the highest final conversion and the slowest (RB-CIHABI) to the lowest final conversion. Moreover, RB-NPG and RB-NPG-CIHABI PIS lead to faster response than SFH⁺-CIHABI. Thus if the maximum polymerization rates R_p are in line with the photochemical reactivity of dyes excited states (i.e. k_q in Table II), it looks more tricky to give a direct relation between final conversions, k_q and photochemical mechanisms. Nevertheless, the two dyes exhibit marked different behaviors for polymerization of the resin under homogeneous irradiation. This result should somehow impact the behaviour of the different PIS used in holographic recording materials where microstructuration at the microscopic scale takes place and gives rise to a stratified polymer at the end of the inhomogeneous exposure.

V- HOLOGRAPHIC RECORDING

These photopolymerizable systems were studied as holographic recording material. The photopatterning was achieved by interference of two coherent plane waves at 514 nm (Fig. 1) and gratings were recorded in transmission geometry, unslanted, with a spatial fringe spacing of 0.9 μm . On illumination, polymerization occurs at different rates in the bright and dark areas. According to the different gradients of concentration, diffusion processes take place from non-light struck areas to the others and a hologram is built by creation of regions with various densities. Permanent thick phase gratings are recorded.

After irradiation, it is possible to open the sandwich and to analyze the free surface polymer. These experiments were performed with an AFM using tapping mode, the aim being the investigation of the polymer matrix at a submicroscopic scale. Typical results are reported in Fig. 3, showing AFM measurements performed at the top surface of the sample.

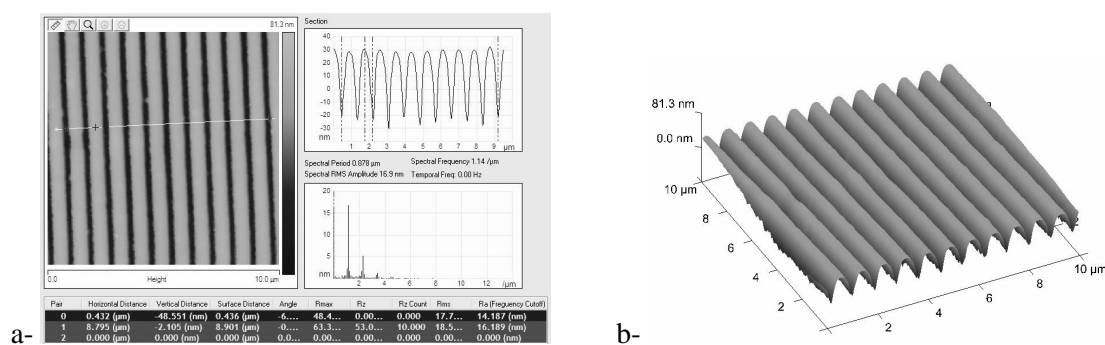


Fig. 3: AFM measurements of the topography of a polymer grating after holographic recording and after removing the glass cover layer: - a: observation of a periodic and regular corrugation illustrated by the 2D profile; - b: 3D reconstruction of the surface.

The topographic analysis shows a surface relief grating corresponding: - to a corrugation mean height of ca 49 nm in the sample; - to a fringe spacing in good agreement with those of the interference pattern (0.87 μm in average determined by AFM). The bright and dark regions corresponding respectively to the polymer-rich and to the monomer-rich regions are observed by the succession of bright and dark stripes in the image. It is in agreement with a mechanism of light induced grating formation linked with molecular migration (mass transport) due to the photochemical

reaction [36], [37] and to polymerization shrinkage [38]. The creation of a surface corrugation after delamination indicates the imperfect compensation of local volume changes in the counterdiffusion process.

The evolution of the diffraction efficiency during illumination inducing grating build-up is displayed in Fig. 4(a) and (b) for RB and SFH⁺ respectively. It is interesting to note that behaviors of 2- and 3-component PIS are different.

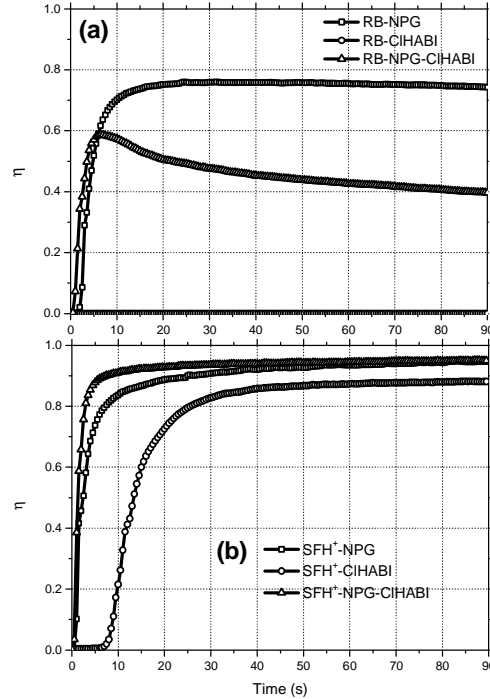


Fig. 4: Evolution of the diffraction efficiency of the different PIS based on RB (a) and on SFH⁺ (b) versus irradiation time at 514 nm with 25 mW/cm² irradiation.

The diffraction efficiency obtained for RB-CIHABI system is always zero (Fig. 4(a)): this system is not able to give rise to a micro-structuration through inhomogeneous irradiation at the microscopic scale, even if polymerization is fulfilled under homogeneous exposure. These results attest that this system is not able to give rise to a significant refractive index modulation: the creation of active radicals is too slow and the polymer chains initiated in the bright areas can easily propagate towards the dark areas, inducing a homogeneous polymerization of the medium in spite of the holographic exposure. The 2-component system RB-NPG leads to final diffraction efficiency around 78%, value higher than that observed for the corresponding 3-component system which is about 40% (cf. Table III). Indeed, the grating curve of the 3-component RB-NPG-CIHABI PIS shows particular shape: i- maximal diffraction efficiency is reached at 60% after 5 s of irradiation; ii- this is followed by a slow decrease of η to achieve 40% after 90s of irradiation (Fig. 4(a)). The degradation of the grating is confirmed by the evolution of the grating formation rates R_η reported on Fig. 5(a) where, after a maximum, R_η of RB-NPG-CIHABI becomes negative before going up toward zero. However, this last shows maximum rate of grating formation around 0.27 s⁻¹ and close to the 0.25 s⁻¹ obtained for RB-NPG system (Fig. 5, Table III). When checking the grating formations rates R_η (Fig. 5(a)), it appears clearly that the RB-NPG PIS leads to a delayed response compared to the RB-NPG-CIHABI PIS: the maximum rate of grating formation is obtained later (around 2.7 and 1.4 s resp.).

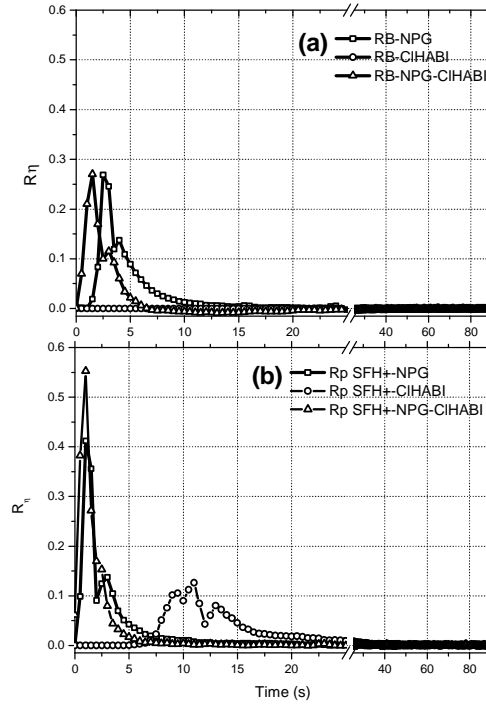


Fig. 5: Evolution of hologram formation R_η for the PIS based on RB (a) and on SFH^+ (b) versus irradiation time at 514 nm with 25 mW/cm^2 irradiance.

The evolution of the diffraction efficiency versus irradiation time of SFH^+ photoinitiating systems are shown in Fig. 4(b). The final diffraction efficiencies and the maximum rate of grating formation are collected in Table III. The middling photopolymerization efficiency observed for the SFH^+ -CIHABI system under homogeneous irradiation leads to final diffraction efficiency around 88%, outperforming the RB-CIHABI system even if an important inhibition time (about 5.5 s) was observed for this system. Furthermore, Fig. 5 shows that the maximum rate of hologram formation is delayed from less than 1 s for SFH^+ -NPG and SFH^+ -NPG-CIHABI to 11 s for SFH^+ -CIHABI, outlining lower reactivity of SFH^+ -NPG and the very bad performance of SFH^+ -CIHABI as photosensitizing material for holographic recording.

The SFH^+ -NPG systems lead to diffraction efficiency close to unity (0.95) and equivalent to the corresponding 3-component PIS RB-NPG-CIHABI. Indeed, CIHABI addition to SFH^+ -NPG increases the maximum rate of grating formation from 0.41 s^{-1} for SFH^+ -NPG system to 0.55 s^{-1} for SFH^+ -NPG-CIHABI (Fig. 5, Table III). As a conclusion, the fastest and more efficient PIS for holographic recording materials is SFH^+ -NPG-CIHABI with both high final diffraction and high maximum rate of hologram formation. In addition, SFH^+ photoinitiating systems are more efficient than the systems based on RB for use of the considered monomer mixture as holographic recording material.

DISCUSSION

Establishment of relations between the performances of the photopolymerizable system in terms of monomer conversion under homogeneous polymerization and those in terms of diffraction efficiency when used in holography is no straightforward matter. Formulating a photopolymerizable recording medium in that case requires a fair knowledge of the coupling between photochemical conversion, polymerization, mass transport and evolution of the matrix viscosity. Physical models taking into account the general mechanism of free radical polymerization are proposed [4], [38], but the approach developed in this paper is different. The aim is to take direct advantage of the polymerization properties of the material.

In order to explain the holographic curves concerning RB systems, another experiment can be introduced concerning the effect of irradiation time on RB-NPG-CIHABI holographic material (Fig.

6): i- when the irradiation was switched off after 3 seconds, the attained value of $\eta = 0.25$ at $t = 3\text{s}$ was kept until the end of the recording; ii- when the irradiation was switched off after 5 seconds, the grating formation is slowed down, η reached a maximum value of 0.48 and very slowly decreased to 0.45; iii- under continuous irradiation, the grating efficiency decreases after 8s from 0.59 to 0.40.

This behavior indicates that for RB systems an efficient polymerization can be induced even in the dark fringes under sustained irradiation, leading to a decrease of the refractive index variation and, consequently, to a lowering of the diffraction efficiency. This phenomenon was already observed in boron-dipyrromethene PIS [25].

On the other hand, giving rise to the lowest final conversion degrees, but best maximum conversion rates and final diffraction efficiencies, the SFH^+ -NPG and SHF^+ -NPG-CIHABI PIS provide fast release of radicals in the medium in enough quantity, leading to very fast initial rates of hologram formation and low inhibition times. In that case, diffusion of monomers from the dark to the bright fringes is promoted. The result is a fast formation of a three-dimensional polymer network in the illuminated areas. This network is propitious to the grating microsineresis process by limiting the diffusion of the living macroradicals toward the dark fringes, but not to the polymerization process because the efficient freezing of the medium corresponds finally to lower monomer conversion degree.

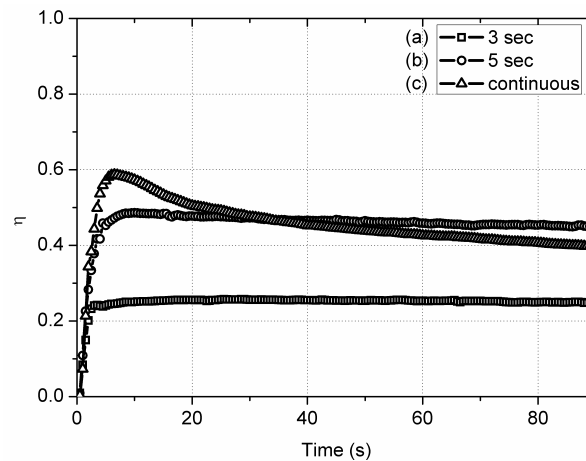


Fig. 6: Evolution of the diffraction efficiency for RB-NPG-CIHABI PIS based holographic material (514 nm with 25 mW/cm^2) during and after exposure: - a: the irradiation is switched off after 3 seconds; - b: switched off after 5 seconds; - c: under continuous irradiation.

CONCLUSION

In this paper, we have demonstrated that the efficiency and sensitivity of holographic recording material is related to the photochemistry of photoinitiating systems. For photoinitiating systems based on same coinitiator, but differing by the dye, the grating formation kinetics was directly related to the properties of the dyes. Finally, we have defined an efficient recording material, based on 3-component PIS, giving rise to thick phase holograms with both high diffraction yield and formation rate.

ACKNOWLEDGMENT

We gratefully thank Dr. Aurélie Chan Yong for gratings recordings and the Optics department at Telecom Bretagne for use of their experimental setup. For these works, the authors acknowledge supports of the project PONANT including funds from Region Bretagne, Etat and Feder.

REFERENCES

- [1] C. Acikgoz, M. A. Hempenius, J. Huskens, and G. J. Vancsoa, "Polymers in conventional and alternative lithography for the fabrication of nanostructures", *Eur. Polym. J.*, vol. 47, pp. 2033-52, 2011.

- [2] Q. He, I. Zaquine, A. Maruani, S. Massenot, R. Chevallier, and R. Frey, “Band-edge-induced Bragg diffraction in two-dimensional photonic crystals”, *Opt. Lett.*, vol. 31, pp. 1184-1186, 2006.
- [3] M. Wang, J. Hiltunen, S. Uusitalo, J. Puustinen, J. Lappalainen, P. Karioja, and R. Myllylä, “Fabrication of optical inverted-rib waveguides using UV-imprinting”, *Microelectron. Eng.*, vol. 88, pp. 175-178, 2011.
- [4] J. Guo, M. R. Gleeson, and J. T. Sheridan, “A review of the optimization of photopolymer materials for holographic data storage”, *Physics Research International*, vol. 2012, ID 803439 (16 pages), 2012.
- [5] H. J. Coufal, D. Psaltis, and G.T. Sincerbox, “Holographic Data Storage”, Springer Series in Optical Sciences: vol. 76, Springer Verlag, New-York, 2000.
- [6] J. P. Fouassier, “Photoinitiation, Photopolymerization, and Photocuring: Fundamentals and Applications”, Hanser Gardner Publications, pp. 388, 1995.
- [7] R. Schwalm, “UV Coatings: Basics, Recent Developments and New Applications”, Elsevier, pp. 322, 2006.
- [8] J. V. Koleske, “Radiation curing of coatings”, ASTM International, pp. 244, 2002.
- [9] R. Bongiovanni, F. Montefusco, A. Priola, N. Macchioni, S. Lazzeri, L. Sozzi and B. Ameduri, “High Performance UV Cured Coatings For Wood Protection”, *Prog. Org. Coat.*, vol. 45, pp. 359-363, 2002.
- [10] P. Coppo, R. Fausto, E. Galoppini, A. Maldotti, M. A. Miranda, K. Mizuno, J. S. Seixas de Melo, N. Serpone, and T. Tsuno, “Photochemistry”, RSC Publishing, pp. 392, 2009.
- [11] W. A. Green, “Industrial Photoinitiators: A Technical Guide”, CRC Press Inc, pp.302, 2010.
- [12] W. Schnabel, “Polymers and Light: Fundamentals and Technical Applications”, Wiley-VCH Verlag GmbH, pp. 396, 2007.
- [13] K. Curtis, L. Dhar, and W.L. Wilson, “Comprehensive Nanoscience and Technology”, Elsevier, vol. 4, pp. 615-630, 2011.
- [14] T. J. Trentler, J. E. Boyd, and V. L. Colvin, “Epoxy resin-photopolymer composites for volume holography”, *Chem. Mat.*, vol. 12, pp. 1431-1438, 2000.
- [15] Y. Qi, M. R. Gleeson, J. Guo, S. Gallego, and J. T. Sheridan, “Quantitative comparison of five different photosensitizers for use in a photopolymer”, *Physics Research International*, vol. 2012, Article ID 975948 (11 pages), 2012.
- [16] J. P. Fouassier, X. Allonas, and D. Burget, “Photopolymerization reactions under visible lights: principle, mechanisms and examples of applications”, *Prog. Org. Coat.*, vol. 47, pp. 16-36, 2003.
- [17] C. Grotzinger, D. Burget, P. Jacques, and J. P. Fouassier, “Visible light induced photopolymerization: speeding up the rate of polymerization by using co-initiators in dye/amine photoinitiating systems”, *Polymer*, vol. 44, pp. 3671-3677, 2003.
- [18] J. P. Fouassier, and E. Chesneau, “Polymérisation induite sous irradiation laser visible, 5. Le système éosine/amine/sel de iodonium”, *Die Makromolekulare Chemie*, vol. 192, pp. 1307-1315, 1991.
- [19] J. P. Fouassier, F. Morlet-Savary, K. Yamashita, and S. Imahashi, “The role of the dye/iron arene complex/amine system as a photoinitiator for photopolymerization reactions”, *Polymer*, vol. 38, pp. 1415-1421, 1997.
- [20] J. P. Fouassier, and S. K. Wu, “Visible laser lights in photoinduced polymerization. VI. Thioxanthenes and ketocoumarins as photoinitiators”, *J. Appl. Polym. Sci.*, vol. 44, pp. 1779-1786, 1992.
- [21] J. He, and E. Wang, “Photoinitiated polymerization by aryliodonium salt/benzophenone/tertiary amine binary photosensitization system”, *Chin. J. Polym. Sci.*, vol. 8, pp. 44-50, 1990.
- [22] X. Allonas, J. P. Fouassier, M. Kaji, M. Miyasaka, and T. Hidaka, “Two and three component photoinitiating systems based on coumarin derivatives”, *Polymer*, vol. 42, pp. 7627-7634, 2001.
- [23] A. Ibrahim, C. Ley, O. I. Tarzi, J. P. Fouassier, and X. Allonas, “Visible Light Photoinitiating Systems: Toward a Good Control of the Photopolymerization Efficiency”, *J. Photopolym. Sci. Technol.*, vol. 23, pp. 101-108, 2010.
- [24] O. I. Tarzi, X. Allonas, C. Ley, and J. P. Fouassier, “Pyromethene derivatives in three-component photoinitiating systems for free radical photopolymerisation”, *J. Polym. Sci., Part A: Polym. Chem.*, vol. 48, pp. 2594-2603, 2010.
- [25] A. Ibrahim, A. Chan Yong, C. Ley, O. Tarzi, C. Carré, and X. Allonas, “Optimization of a photopolymerizable material based on a photocyclic initiating system using holographic recording”, *Photochem. Photobiol. Sci.*, vol. 11, pp. 1682-1690, 2012.
- [26] M. De Sarkar, J. Qi, and G.P. Crawford, “Influence of partial matrix fluorination on morphology and performance of HPDLC transmission gratings”, *Polymer*, vol. 43, pp. 7335-7344, 2002.
- [27] M. D. Schulte, S. J. Clarson, L. V. Natarajan, D. W. Tomlin, T. J. Bunning, “The effect of fluorine-substituted acrylate monomers on the electro-optical and morphological properties of polymer dispersed liquid crystals”, *Liquid Crystals*, vol. 27, pp. 467-475, 2000.
- [28] C. Carre, R. Chevallier, B. Mailhot, and A. Rivaton, “Understanding microstructure development in holographic polymer-dispersed liquid crystals”, in “*Basics and applications of photopolymerization reactions, vol. 3*”, J.P. Fouassier, X. Allonas, Eds.; Research Signpost: Trivandrum, pp. 175-84, 2010.

- [29] S. Massenet, R. Chevallier, J.-L. de Bougrenet de la Tocnaye, and O. Parriaux, "Tunable grating-assisted surface plasmon resonance by use of nano-polymer dispersed liquid crystal electro-optical material", *Opt. Com.*, vol. 275, pp. 318-323, 2007.
- [30] T. M. Roper, T. Kwee, T. Y. Lee, C. A. Guymon, and C. E. Hoyle, "Photopolymerization of pigmented thiol-ene systems", *Polymer*, vol. 45, pp. 2921-2929, 2004.
- [31] C. Decker, and K. Moussa, "Real-time kinetic study of laser-induced polymerization", *Macromolecules*, vol. 22, pp. 4455-4462, 1989.
- [32] A. Ibrahim, V. Maurin, C. Ley, X. Allonas, C. Croutxe-Barghorn, and F. Jasinski, "Investigation of termination reactions in free radical photopolymerization of UV powder formulations", *Eur. Polym. J.*, 2012, vol. 48, pp. 1475-1484 (2012).
- [33] P. Hariharan, *Optical holography, Principles, Techniques and Applications*, Cambridge University Press, Cambridge, 1984.
- [34] D. Rehm, and A. Weller, "Kinetics of fluorescence quenching by electron and hydrogen-atom transfer", *Isr. J. Chem.*, vol. 8, pp. 259-265, 1970.
- [35] X. Allonas, J. P. Fouassier, M. Kaji, and Y. Murakami, "Excited state processes in a four-component photosensitive system based on a bisimidazole derivative", *Photochem. Photobiol. Sci.*, vol. 2, pp. 224-229, 2003.
- [36] A. Mazzuella, P. Pagliusi, C. Provenzano, G. Russo, G. Carbone, and G. Cipparrone, "Surface relief gratings on polymer dispersed liquid crystals by polarization holography", *Appl. Phys. Lett.*, vol. 85, pp. 2505-2508, 2004.
- [37] H. Ono, A. Hatayama, A. Emoto, and N. Kawasutuki, "Migration induced reorientation and anisotropic grating formation in photoreactive polymer liquid crystals", *Opt. Mater.*, vol. 30, pp. 248-254, 2007.
- [38] Y. Tomita, K. Chikama, Y. Nohara, N. Suzuki, K. Furushima, and Y. Endoh, "Two-dimensional imaging of atomic distribution morphology created by holographically induced mass transfer of monomer molecules and nanoparticles in a silica-nanoparticle-dispersed photopolymer film", *Opt. Lett.*, vol. 31, pp. 1402-1404, 2006.
- [39] M.R. Gleeson, J. Guo, and J.T. Sheridan, "Optimisation of photopolymers for holographic applications using the Non-local Photo-polymerization Driven Diffusion model", *Opt. Exp.*, vol. 19, pp. 22423-22436, 2011.